CLM - P 521

CLM - P 521

UKAEA

Preprint

ELECTRON DENSITY MEASUREMENTS USING THE STARK BROADENED LINE WINGS OF HYDROGENIC IONS IN LASER PRODUCED PLASMAS

C C SMITH
N J PEACOCK

CULHAM LABORATORY
Abingdon Oxfordshire

1978

CLM - P521

ELECTRON DENSITY MEASUREMENTS USING THE STARK BROADENED LINE WINGS OF HYDROGENIC IONS IN LASER PRODUCED PLASMAS

By

C.C. Smith* and N.J. Peacock
Culham Laboratory, Abingdon, Oxon OX14 3DB U.K.
(Euratom/UKAEA Fusion Association)

ABSTRACT

It is shown that the measurement of wing intensities of those Stark broadened Lyman lines, for which the upper level is thermally populated with respect to the free electrons and fully stripped ions, enables accurate deduction of electron density in high temperature plasmas. The parameters which characterise the plasma microfield distributions are defined in such a way as to allow the use of existing tabulated values of the electric microfield to construct accurate theoretical profiles. The method is illustrated using emission lines from laser-irradiated solid polymer targets. Analysis of the broadening of CVI resonance lines yields values of electron density about a factor of two higher than the critical density, $\sim 10^{21}$ cm^{-3}, for reflection of the incident laser beam.

(Submitted for publication in J.Phys.B., Atom. Molec. Phys.)

* On attachment from Imperial College, London.

January 1978

CMS

1. INTRODUCTION

Analysis of the emission spectra of highly-stripped ions from the core of laser-imploded pellets is potentially the most direct and reliable method for deducing the ultra-high-pressure plasma conditions. It is no simple matter, however, to extend the well established visible and near U.V. techniques, used for less dense, cooler plasmas, into the soft X-ray region where these ions emit. This paper describes an accurate method of density measurement which is particularly suitable for plasmas consisting mainly of singly charged ions, for example, where highly charged hydrogenic ions are present only as a small impurity in a deuterium plasma.

Attempts have been made in the past, mainly using plasmas produced at plane targets, to demonstrate the feasibility of exploiting various features of the emission spectra for plasma diagnostics. With regard to density determinations, however, success has been very limited largely because of inherent shortcomings of the method employed. Thus density deductions based on intensity measurements of recombination continua (see e.g. Galanti and Peacock 1975) suffer from the inherent inaccuracies associated with the need for: (i) absolute intensity calibration of the detection system, (ii) detailed knowledge of the spatial and temporal extent of emission from the plasma within the acceptance of the detection system, (iii) precise knowledge of the ionisation balance and relative population of the particular ionic species being observed.

Spectral line shapes would seem to offer a probe of plasma conditions free from these limitations. Frequently the lines are optically thick so that accuracies are limited by the need to know spatial distributions of both the ground state and upper state number densities throughout the plasma in the line of sight of the detection system. A further complication near line centre is that ion motions may dominate the broadening. Line profiles showing asymmetric self reversals due to cooler outer regions of plasma and the mass motion (streaming) of the ions are fairly typical, particularly in plane

target experiments. Such profiles have been explained schematically by Irons (1975), although his model calculations are not necessarily related to any real physical situations. It is apparent, therefore, that analysis of the line centre does not provide a useful diagnostic without independent measurement of the spatial distribution throughout the plasma of either the line source function or the ions' velocity distribution. At best, assuming the validity of some plasma modeling, such analysis of the line shapes can only yield information on the velocity and excitation distributions of the emitting ions rather than their plasma environment.

For high series members having smaller optical depth, Stark broadening can become sufficiently important to allow an accurate derivation of particle density(see for example, the CVI Ly-γ profile presented by Peacock 1976).

This paper examines the possibility of making measurements solely on the line wings. This portion of the line is necessarily optically thin and densities may be deduced directly since the broadening depends only on the ion-produced electric microfield. Theoretical variations in wing intensity with changes in density are compared with experimental profiles in order to demonstrate the sensitivity of the method and thus the accuracy of the result. The method is generally applicable to high temperature plasmas where simple modifications to published microfield distributions allow the prediction of reliable theoretical profiles without the need for complex calculations. The effects of Debye screening and radiator-perturber correlations are incorporated by suitable choice of the parameters which characterize the distribution. The parameter regime within which accurate predictions are to be expected is shown to include electron densities as high as 3.10^{24} cm^{-3}. Normalisation of the observed profiles is achieved by reference to the intensity of the free-bound continuum at the series limit. A high temperature is again useful, here, since Boltzmann factors relating upper state populations to the free electron number density become insensitive to temperature.

2. MICROFIELD DISTRIBUTIONS

Sophisticated and accurate calculations by Hooper (1968a) characterized the electric microfield distribution in terms of a screening parameter a, defined by

$$a = \frac{r_o}{\lambda_D} \tag{1}$$

where $r_o = \left(\frac{1}{\frac{4}{3} \pi N_e} \right)^{\frac{1}{3}}$ and $\lambda_D = \left(\frac{kT_e}{4\pi N_e e^2} \right)^{\frac{1}{2}}$

Field strengths were specified in units of a reduced field strength ε_o, given by

$$\varepsilon_o = \frac{e}{r_o^2} \tag{2}$$

The case $a = 0$ was not tabulated by Hooper, being identical with the Holtsmark distribution.

For sufficiently high temperatures, microfield distribution functions necessarily tend toward the Holtsmark limit for any plasma, independent of the charge state. That is, for $a = 0$ the probability distribution of the field strength, expressed in units of the normal field strength, F_o, is as given by Holtsmark (1919)

$$F_o = 2.603 \; Z_p e \; N_p^{\frac{2}{3}}$$

where Z_p is the charge and N_p the number density of the (perturbing) ions of the plasma. A similar dependence on Z_p and N_p may be introduced into Hooper's reduced field strength by defining

$$E_o = \frac{Z_p e}{r_p^2} \tag{3}$$

where

$$r_p = \left(\frac{1}{\frac{4}{3} \pi N_p} \right)^{\frac{1}{3}}$$

(This only differs by a factor of the order of unity from the Holtsmark normal field). For plasmas consisting entirely of singly charged ions this definition is identical with equation(2). When ions of greater charge are included, however, there arise significant differences and, from the point of

view of examining the deviations from Holtsmark at $a > 0$, equation (3) is the appropriate choice. These deviations occur because the Holtsmark treatment calculates the probability of each perturber configuration neglecting all ion-ion correlations and does not allow that the field produced by any given perturber configuration is reduced by Debye screening. The latter effect, fully allowed for by Hooper, does not depend on the charge state of the ions. i.e. the reduction in the field produced by a given perturber configuration depends only on the value of the Debye length. Thus a single parameter may be used to characterise modifications to the Holtsmark distribution due to Debye screening if the screening length, λ_D, is related to the perturber configurations themselves, i.e. to perturber separations. We define, therefore a screening parameter a' by

$$a' = \frac{r_p}{\lambda_D} \qquad (4)$$

Again this reduces to Hooper's definition for Zp = 1.

The re-parameterisation given by equations (3) and (4) is not trivial for $Z_p > 1$. The results of O'Brien and Hooper (1972), plotted in terms of ε_o for various values of a as defined by equations (1) and (2), show distributions which are sensitive to the value of Z_p. This approach tends to be somewhat misleading from the point of view of examining deviations from Holtsmark. Meaningful comparisons may only be made with field strengths defined in terms of E_o (equation 3) at given values of a' (equation 4). Fig. 1a illustrates the effect of such a rescaling of the microfield distributions at a singly charged point in a plasma of doubly charged ions. We use,

$$W(\beta)\ d\beta = P(\varepsilon)\ d\varepsilon$$

where $W(\beta)$ is the probability distribution of the field strength measured in units of E_o. $W(\beta)$ is derived from O'Brien and Hooper's tabulated values of $P(\varepsilon)$ and plotted for a values of 0.2 and 0.6. According to equation (4), these a values correspond to values of a' of 0.25 and 0.76 respectively. The $W(\beta)$ distributions are shown compared with curves for the same values of a' for a plasma of singly charged ions (obtained by interpolation from Hooper's

(1968a) values). Nearly identical distributions are seen to result.

Use of the parameter a' which properly accounts for Debye screening of ion produced fields, is in itself insufficient to yield accurate results when ion charges become much bigger. It is, of course, also necessary to account for changed probabilities of any given perturber configuration due to ion - ion interactions. Even for these correlation effects, however, a' is a much more useful parameter than a since much of the Z_p dependence of the distribution is then removed. A simple illustration of this fact is obtained by considering the asymptotic regime where nearest neighbour theory may be used to estimate the effect of correlations. We are here concerned with radiator-perturber correlations in a regime where they exert their greatest influence. The probability for the radiator-perturber separation is given by:-

$$W(r)dr = 4\pi r^2 N_p g(r) dr$$

where g(r) is essentially a Boltzmann factor weighting the probability according to the interaction energy compared with thermal energies

i.e. $$g(r) = \exp - \left\{ \frac{(Z - 1) Z_p e^2}{rkT_e} e^{-\frac{r}{\lambda_{D'}}} \right\}$$

Z-1 is used for the ion charge in keeping with the tradition that Z represents the core charge of a radiating ion. A Debye screened interaction potential is used (in Debye-Huckel theory g(r) corresponds to the two particle correlation function) requiring a screening radius

$$\lambda_{D'} = \left(\frac{kT_e}{4\pi (N_e + Z_p^2 N_p) e^2} \right)^{\frac{1}{2}} .$$

With a screened field

$$E = \frac{Z_p e}{r^2} \left(1 + \frac{r}{\lambda_D}\right) e^{-\frac{r}{\lambda_D}}$$

defining $x = \frac{r}{r_p}$ and $\beta = \frac{E}{E_o}$, we have,

$$g(r) = \exp - \left\{ \frac{(Z-1) a'^2}{3x} e^{-(1+Z_p)^{\frac{1}{2}} a' x} \right\} \qquad (5)$$

and $\beta = \frac{1}{x}2 \quad (1 + a' \; x)e^{-a'x}$

giving $W(\beta)d\beta = 3x^2 \exp - \left\{\frac{(Z-1)a'^2}{3x} \quad e^{-(1+Z_p)^{\frac{1}{2}}a'x}\right\} dx$

i.e. $$W(\beta) = \frac{3x^4 \exp - \left\{\frac{(Z-1)a'^2}{3x} \quad e^{-(1+Z_p)^{\frac{1}{2}}a'x}\right\}}{a' \left(2 + \frac{2}{a'x} + a'x\right) e^{-a'x}}$$

which is exactly equivalent to asymptotic expressions in Hooper (1968b) and O'Brien and Hooper (1972). The important feature to notice when cast in this form is the very weak dependence of Z_p; indeed for strong fields, as x tends to zero, the Z_p dependence disappears altogether.

At smaller values of β the pair correlation function influences the distribution in a much more complicated way. Approximate estimates may be obtained by the simple procedure of using equation(5) to rescale Hooper's (1968a) values at the appropriate value of a'. The radiator-perturber correlations for $Z_p = 1$ must first be removed, however, and the rescaling carried out over the whole distribution to allow renormalisation of the integrated probability to unity.

This approach needs some justification since at small β ($\beta<10$), the microfield is definitely not due to a single perturber and, what at first sight may seem more serious, the Z_p dependence increases as β decreases. At small β, however, the correction to the probability of any perturber configuration due to radiator-perturber correlations is, in itself, only very small. This is illustrated in Fig. 1b and 1c where distributions are shown for the a' values of 0.6 and 0.8 respectively, for several values of Z_p. At smaller values of a' changes in Z_p cause insignificant changes in the distribution so that the question of the accuracy of the correction does not arise. At large a' ($\sim$0.8) corrections $\sim$10% are to be expected for $\beta<10$ and for moderate values of Z_p (10-20). Even allowing that the method of correction is not very accurate, therefore, errors still of the order of only a few per cent may be expected.

It is interesting to note from equation 5 the direction of the change in corrections due to radiator-perturber correlations as Z_p increases, i.e. the effect of correlations is reduced at higher Z_p (at a given value of a'). This may be understood physically in terms of the definition of a' which relates the electron screening distance, λ_D, of ion produced fields to ion separations, r_p. For a given value of a', therefore, the screening radius appropriate to ion-ion interaction energies, λ_D', shows a relative decrease as Z_p increases (i.e. stronger screening, or weaker interaction).

Perturber - perturber correlations must also become increasingly important as Z_p increases. Here the pair correlation function depends on Z_p^2 rather than $(Z-1)Z_p$. Working in terms of a' only removes one of the Z_p's; one must remain, just as the (Z-1) remains in equation (5). In a plasma of singly charged ions, however, perturber-perturber correlations are bound to remain only a small correction. Indeed, for $Z_p \sim Z-1$ the method of Hooper (1968a) indicates that perturber-perturber correlations generally give an insignificant correction compared with the radiator-perturber interaction. (Hooper gives two approximations to the microfield probability distribution, which everywhere differ by less than 2%. Only the second has terms depending on non-central interactions). If the correction for radiator-perturber correlations (equation 5) is small, therefore, no other corrections are required.

The correction indicated by equation (5) is not expected to be accurate at small values of β. It is necessary again, therefore, to ensure that equation (5) only gives a small correction so that no serious inaccuracy results in the corrected distribution. This may only be satisfied as Z becomes large (because of the presence of the (Z-1) term) by restricting a' to small values. Within the parameter regime

$$(Z-2)a'^{2} \lesssim 0.3 \qquad (6)$$

i.e. $$\frac{(Z-2)\, Z_p^{\frac{2}{3}}\, N_e^{\frac{1}{3}}}{T_e} \lesssim 5.10^6, \quad T_e \text{ in eV} \quad ,$$

distributions can be calculated which nowhere are inaccurate by more than a few per cent. The Z-2 term appears since Hooper's calculations already allow for Z-1 = 1. If equation(6) is satisfied the correction at small β is generally small, rising to less than 10% by $\beta = 6$ and $\sim$ 15% by $\beta = 10$. Beyond this the correction becomes increasingly accurate.

The temperature at which ions appear in plasmas generally scales $\sim Z^2$. We make use of this in Fig. 2 to plot the validity region of equation (6) in terms of density and emitter charge state. Clearly the range of validity is widest in a plasma of singly charged ions. A scaling of $kT_e = Z^2 Ry$ is assumed which is typical of the non-stationary plasmas formed at irradiated plane solid targets. In plasmas with a stationary ionisation balance, $kT_e \sim Z^2$ Ry/5 is commonly experienced. This would result in a decrease in the upper density limit shown in Fig. 2 by some two orders of magnitude for the 'high temperature' approximation to remain valid. (At higher densities the method does not become impossible but the accuracy is bound to get worse).

3. MEASUREMENT OF EXPERIMENTAL PROFILES

Plasmas were formed by laser irradiation of plane polythene and P.T.F.E. targets. Power densities of 2.10^{14} W.cm^{-2} were delivered on target by focussing the output of a Nd doped glass laser through a single element, aspheric Soro lens. The laser was operated at a power level $\sim$ 20 GW, delivering 40 J in a pulse of $\sim$2 nsec duration.

Spectra were recorded photographically in the wavelength range 4 - 50 Å using a GML 5 spectrograph* fitted with a holographically produced 600 line/mm grating and with a 3 µm entrance slit. At this slit width the instrumental function had full width $\sim$ 0.01 Å. Spatial resolution was achieved by means of a second slit placed perpendicular to the entrance slit just in front of the grating. Fig. 3 illustrates the spectrum integrated over 8 irradiation pulses on a P.T.F.E. target, while the spectrum from 4 pulses on a polythene target is shown in Fig. 4.

* Supplied by Grating Measurements Ltd., London.

Usually it is advantageous for the second slit to be as narrow as possible resulting in some partial equivalence of spatial and temporal resolution. For the purposes of the present experiment, however, this is hardly a consideration since we are specifically concerned with the very hot, dense region close to the critical surface in the plasma where most of the energy is absorbed. It is clear from the portions of spectra shown in Figs. 3 and 4 by the abrupt cut-off away from the target surface of the intense free-bound continua and satellite line emission that this is a very narrow spatial region. Indeed, previous work (Galanti and Peacock 1975) has indicated the thickness of this layer to be no greater than a few microns. Even if such fine spatial resolution were to be used, interpretation would still be complicated by the possibility of movement of the critical surface within the time duration of the laser pulse.

In this paper we rely on the fact that an extremely short heating time, $\sim 10^{-11}$ sec, of the plasma results in the establishment of an almost constant density profile within the much longer duration of the laser pulse (Galanti and Peacock 1975). Mass motion and subsequent rapid cooling of the expanding plasma ensure that the high temperature continuum intensity arises almost entirely from the highest pressure region. The continuum emission provides diagnostic information for interpretation of the line profiles. It was necessary, therefore, to take the line profile data from the same spatial region of plasma. Microphotometer scans were taken along a narrow strip of that part of the photographic image of the space resolved spectrum shown in Figs. 3 and 4 as corresponding to the target surface. Exposure here could only be caused by the high pressure region of plasma. Further from the target surface (at distances shown as greater than zero mm in Figs 3 and 4) other regions of plasma could also contribute.

4. DISCUSSION OF LINE PROFILES

In the approximation that the intensity of emission at any frequency, ν, in the line wing is proportional to the probability of a plasma microfield which would give a shifted component in the Stark pattern of the line at $\nu = CE$, the lineshape function is given by

$$L(\nu) = \frac{K}{CE_o} W(\beta) \qquad (7)$$

Values of C, with suitable Z scaling, may be derived from 'asymptotic Holtsmark coefficients' given by Griem (1974). K is a normalisation constant such that $\int L(\nu)d\nu = 1$ (since $\int W(\beta)d\beta = 1$, for Lyman α, which has an unshifted component containing two thirds of the intensity of the line, we have $K = \frac{1}{6}$; for Lyman β with no unshifted component, $K = 0.5$; and for Lyman γ, having an unshifted component of 26.6%, $K = 0.367$). The approximation is justified for the region of the line being studied where electron, Doppler and instrumental effects represent insignificant corrections.

Fig. 5 shows microdensitometer traces of lower members of the CVI Lyman series with theoretical profiles calculated from

$$D(\nu)\ d\nu = N_n\ A_{nl}\ \frac{h\nu}{4\pi}\ L(\nu)\ d\nu\ G(\nu) \qquad (8)$$

where $G(\nu)$ depends on the detection geometry, plasma dimensions and emission time and sensitivity of the spectrograph and photographic plate. $L(\nu)$ is derived as above with $W(\beta)$ calculated according to the method of §2, suitable averages being taken to allow for several perturber species. The values of a' used were 0.13 for polythene and 0.18 for P.T.F.E., as calculated from the values of the particle densities given in §5, and are seen to be well within the bounds set by equation (6).

An absolute intensity calibration is implied by use of equation (8). In practice the wing intensity was placed on an absolute basis by scaling the theoretical profiles according to the observed level of the free-bound continuum emission at the series limit. The density on the photographic plate caused by this continuum is given by

$$D(\nu)\, d\nu = 2.8\ 10^{-57}\ \frac{Z^4\, N_e\, N_i}{(kT_e)^{\frac{3}{2}}}\ \exp\left(\frac{\chi_i - h\nu}{kT_e}\right) d\nu\ G(\nu) \qquad (9)$$

where kT_e is in ergs and χ_i is the ionisation energy into state i, the fully stripped ion. All that is required, therefore, is a small correction in the $G(\nu)$ factor for the relative response of the detection system over the small wavelength range from the series limit to the wavelengths of the lines. Due to the high temperature, $kT_e > \chi_i$, the exponential fall off of the continuum beyond the CVI series, Fig. 4, is only very slight. It is a reasonable procedure to extrapolate back to the series limit and ignore the exponential altogether. The continua beyond the FIX and FVIII series at shorter wavelengths, shown in Fig. 3, do show a noticeable fall off and, in fact, provide a good temperature diagnostic, a value $\sim (1 \pm 0.3)$ keV being deduced.

We can now specify all the unknowns, except $L(\nu)$ on the right hand side of equation(8) by involving equation (9) for the free bound intensity with the level populations, N_n, given by Saha's equation:

$$\frac{N_e\, N_i}{N_n} = \left(\frac{2\pi\, mkT_e}{h^2}\right)^{\frac{3}{2}}\ \frac{1}{n^2}\ \exp - \frac{\chi_{in}}{kT_e}$$

where χ_{in} is the ionisation energy out of level n. The only remaining dependence on temperature is in the exponential term which, for $kT_e >> \chi_{in}$ causes very little uncertainty even for a relatively crude temperature measurement.

We need to justify the use of Saha's equation. Validity criteria based on collisional-radiative (steady state) models for a level n to be thermally populated with respect to the next higher ionisation stage and the free electrons, see e.g. McWhirter (1965), are not applicable to the plasma situation of this experiment. Here the ionisation balance is determined by the time taken for the ions to stream through a very narrow ionising layer. The relevant question, therefore, is whether excitation and ionisation rates are fast enough, compared with the time the ion remains in the ionising

region, for that level not to remain overpopulated with respect to the levels above it. Ground states typically remain overpopulated by about two orders of magnitude compared with steady state models, Galanti and Peacock (1975). Criteria for thermal population of excited levels, therefore, require a plasma model in which electron parameters, ion velocities and ionisation depths are specified.

In the present experiment a more direct method, based on observation, is available. This is provided by the portion of spectrum shown in Fig. 3 where measurement of intensities of the FIX Lyman lines relative to the continuum at the series limit allows deduction of the quantum level above which a thermal population prevails. Within experimental error, population ratios are measured at L.T.E. values down to and including n = 3. The lower series members require a correction for optical depth but observation of the continuum beyond the FVIII resonance series limit allows sufficiently accurate determination of the FIX n = 1 population. The binding energy of the n= 3 level of FIX is almost the same as that of the n = 2 level of CVI whence their departure from L.T.E. should be similar. Even stronger evidence is provided in the FIX Lyman α line which remains saturated to a point in the profile where the broadening may be accurately determined, being due entirely to quasi-static ions. The optical depth correction is, here, reasonably accurate. The corrected intensity indicates an over-population of the n = 2 level, relative to its L.T.E. value, of between 50% and 100%. With the strong dependence of collision induced transition rates on energy differences we are therefore confident in assuming a sufficient rate upwards out of the n = 2 level of CVI for a thermal population to be well established.

Theoretical profiles are shown in Fig. 5 corresponding to different values of E_o demonstrating how the experimental wing intensity allows a unique determination of E_o, and thence N_e (see § 5). Thus too small a value of E_o gives a prediction of far wing intensity lower than observed, while

too high an E_o does the opposite (except where optical opacity reduces the observed intensity below the predicted curve near line centre for Lyman α and Lyman β). (Widely spaced values of E_o have been deliberately chosen to illustrate this effect). For Lyman γ, we see in Fig. 5 that the addition of a central component (having 26.6% of the area) would give predicted curves having about the same area as the observed profile - i.e. the line is optically thin. Various features of the spectra cause some uncertainty in the choice of the best fit value of E_o for individual lines. Satellite emmission appears on the long wavelength side of Lyman α with the CVI $1s^2$ - 1s4p transition (mainly in absorption) on the short wavelength side. The Lyman δ wing is superimposed on the short wavelength side of Lyman γ, and a second order FVIII line on the long wavelength wing of P.T.F.E. Lyman β. Even so, taking the three lines for each plasma as a whole there can be little doubt that, of the values shown for E_o, 4.10^5 c.g.s. field strength units is the most appropriate for the P.T.F.E. plasma and 3.10^5 for polythene. It is also clear that these values should be accurate within finer limits than set by the widely spaced values of E_o shown in Fig. 5; even allowing for experimental uncertainty in the measurement of the continuum step a certainty within 20% should be attainable with no great difficulty. Since this work is intended primarily to demonstrate the method, however, a more detailed analysis in finding a best fit value of E_o is not presented.

5. DERIVATION OF ELECTRON DENSITY

In direct generalisation of equation (2) we write

$$E_o = \left(\frac{4}{3}\pi\right)^{\frac{2}{3}} e \left(\sum Z_p^{\frac{3}{2}} N_p\right)^{\frac{2}{3}} . \qquad (10)$$

To determine N_e from $N_e = \sum Z_p N_p$ (11)

as well as knowing E_o, we need to know the population of the various ionisation stages. Furthermore, in determining E_o, a value of a' was required for predictions of the profiles, and a' depends on actual perturber number densities. When it is realised, however, that the Z dependence of equations (10) and (11) almost cancels and that, in terms of N_e, the density dependence of equation (4) is very slight ($\sim N_e^{\frac{1}{6}}$) it is clear that no lengthy process is involved in obtaining self consistent values.

Since upper levels are closely tied to the free electron density, while ground states are excessively overpopulated, no serious error is introduced by assuming the total number density of each ionisation stage to be given by the ground state number density. The relative intensities of continua at the various series limits therefore directly allows deduction of the relative populations of the various ionisation stages. Thus from the absence of continuum at the CV series limit, in both polythene and P.T.F.E., we deduce that carbon ions exist almost entirely as fully stripped ions ($Z_p = 6$). In P.T.F.E. the continua at the FIX and FVIII series indicates a relative population of F^{9+} to F^{8+} in the ratio 1:4. No continuum is available for the deduction of the relative F^{7+} population (but as will be seen below uncertainty in this quantity causes little inaccuracy in the density deduction). We may assume $N(F^{7+})$ to be somewhat lower than $N(F^{8+})$; both from the fact that since substantial burn through to F^{9+} has occurred we expect F^{8+} to be dominant and from the observation that the FVIII lines are weaker than FIX lines at the same value of n .

The table overleaf summarises the relative populations. Plasmas (a) and (b) both refer to the P.T.F.E. plasma and represent extreme situations to allow for the uncertainty in $N(F^{7+})$. Case (c) refers to the polythene plasma. Populations are expressed as fractions of N_e, the denominators being those required to satisfy equation (11). The ratios for the different elements are in accord with the initial chemical composition of the target material

Z_p	9	8	7	6	1
a	$\frac{1}{56}$	$\frac{4}{56}$	-	$\frac{2.5}{56}$	-
b	$\frac{1}{96}$	$\frac{4}{96}$	$\frac{4}{96}$	$\frac{4.5}{96}$	-
c	-	-	-	$\frac{1}{8}$	$\frac{2}{8}$

Inserting these values into equation (10) and comparing with the observed values of E_o we derive the values:-

$$E_o = \begin{matrix} a & b & c \\ 1.99 & 1.93 & 1.63 \end{matrix} \times \left(\frac{4}{3}\pi\right)^{\frac{2}{3}} e N_e^{\frac{2}{3}} \text{ c.g.s. units.}$$

giving $N_e = 2.0 \quad 2.1 \quad 1.8 \times 10^{21} \text{ cm}^{-3}$.

It is interesting to note that the derived value of N_e is approximately the same for the two plasmas while ion densities show a considerable difference. We have independent evidence to this effect from a comparison of the intensities between the two plasmas of the continua beyond the CVI series, which depend on the product $N_e N(C^{6+})$. Since $N(C^{6+})$ is known as a fraction of N_e the observed relative intensity depends on the ratio of the values of N_e^2 in the two plasmas. Allowing for the fractional abundance of $N(C^{6+})$ in each plasma, and for the different photographic plate exposures, the observed relative intensity corresponds to N_e being the same, in each plasma, to within the accuracy of measurement ($\sim$10%). One further interesting point is that the above value for the electron density associated with the highest pressure region is within the range of values deduced at lower laser irradiation intensities by quite separate diagnostic methods, Peacock (1976).

6. CONCLUSIONS

Members of the Lyman series of CVI have been observed from laser produced plasmas and their wing intensities interpreted as being due to Stark broadening caused entirely by quasi-static ions.

Parameters have been defined which allow the use of existing tabulated values for accurate prediction of ion microfield distributions in plasmas containing multiply charged ions.

A plasma regime has been identified in which the intensity of optically thin portions of the line (relative to the free-bound continuum beyond the series limit) depends only on the line shape function. Within this regime the line shape analysis thus becomes independent of all plasma parameters except the ion (perturber) density which, consequently may be accurately deduced. The electron density follows immediately from the relative abundances of the ion species which manifest themselves by their respective free-bound continuum intensities.

Values of N_e about a factor of two higher than the critical density for reflection of the incident laser radiation have been deduced for the hottest spatial region of the plasmas produced at targets of both P.T.F.E. and polythene.

The result of the measurement of electron density is, in itself, of some significance in understanding the heating of the plasma by the incident laser radiation. More important in the context of this paper is the suggested accuracy (20 -30%) with which the measurement can be made in plasmas such as were observed in the experiment described in the paper. To the authors knowledge, no previous measurement of $N_e \gtrsim 10^{21} cm^{-3}$ has been made with this accuracy in a laser produced plasma. The method is directly extrapolable to multi-beam laser compression experiments in which densities of the order of the solid state can be reached.

7. ACKNOWLEDGEMENTS

Thanks are due to Mr. A.H. Jones for maintaining and operating the laser. We gratefully acknowledge comments from Dr. D.D. Burgess, Dr. R.W. Lee and Mr. H. Gordon, on preliminary versions of this paper.

REFERENCES

Galanti M. and Peacock N.J. 1975, J. Phys. B, 8, 2427-2447.

Griem H.R. 1974, 'Spectral Line Broadening by Plasmas' (N.Y. Academic Press).

Holtsmark J. 1919, Ann. Phys., 58, 577.

Hooper C.F. 1968a, Phys. Rev., 165, 215-222.

" 1968b, Phys. Rev., 169, 193-195.

Irons F.E. 1975, J. Phys. B, 8, 3044-3068.

McWhirter R.W.P. 1965 'Plasma Diagnostic Techniques' (N.Y. Academic Press) Chap.5.

O'Brien J.T. and Hooper C.F. 1972, Phys. Rev. A, 5, 867-884.

Peacock N.J. 1976, 'Beam Foil Spectroscopy' Vol 2. (N.Y. Plenum), 925-950.

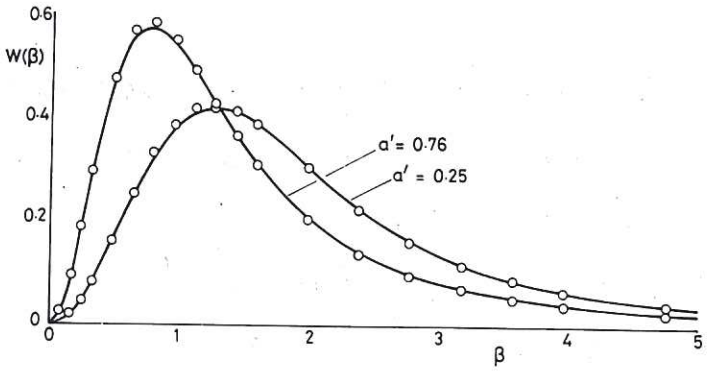

(a)

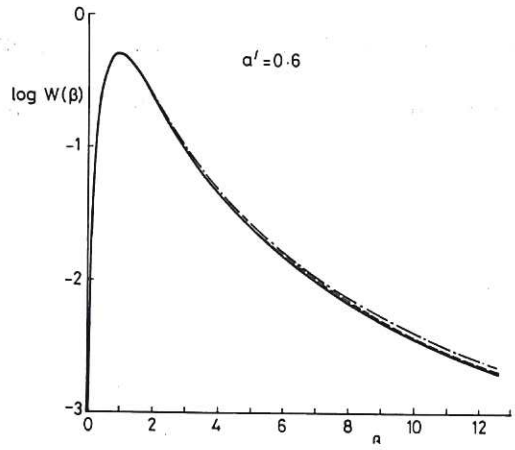

(b)

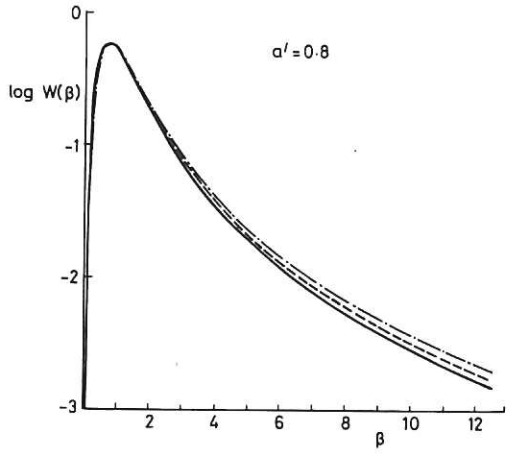

(c)

Fig.1 Microfield distributions at a singly charged point for values of a' as shown. Full curves (taken from Hooper 1968a) represent values for a plasma of singly charged ions i.e. $Z_p = 1$. (a) Open circles (from O'Brien and Hooper 1972) represent values for a plasma of doubly charged ions i.e. $Z_p = 2$. (b) Dashed curves represent values (see text) at $a' = 0.6$, for higher values of Z_p:– – – $Z_p = 10$; —·—·— $Z_p = 30$. (c) as (b) except $a' = 0.8$.

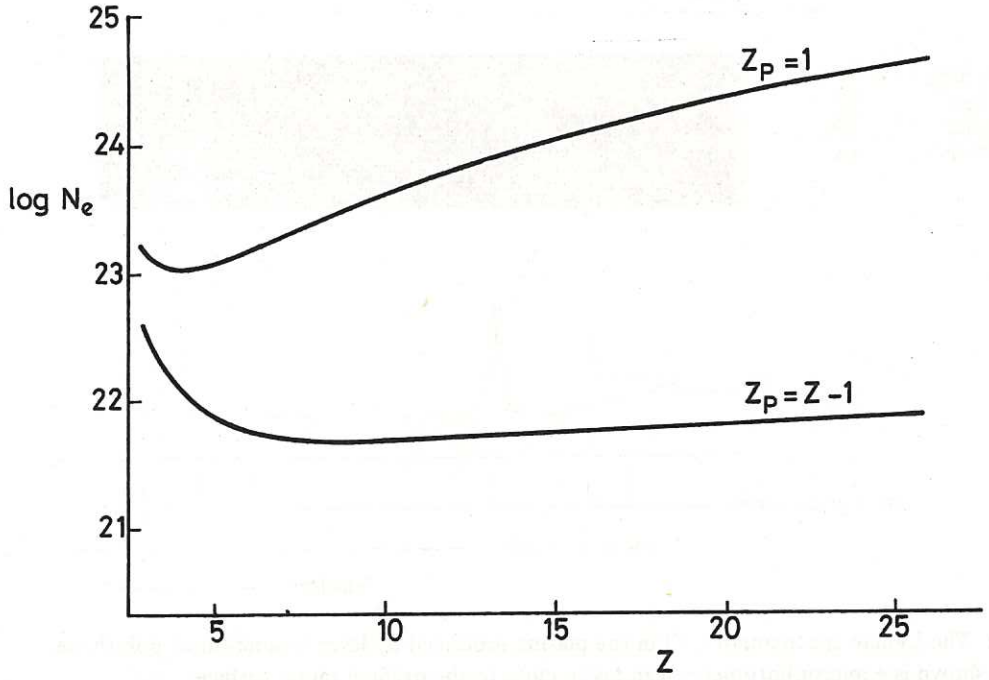

Fig.2 Regions of validity of equation (6) for plasmas with $Z_p = 1$ and $Z_p = Z - 1$ as indicated. For an ion of a given Z (in a plasma with $kT_e = Z^2 Ry$) equation (6) is valid at any density below the solid curve.

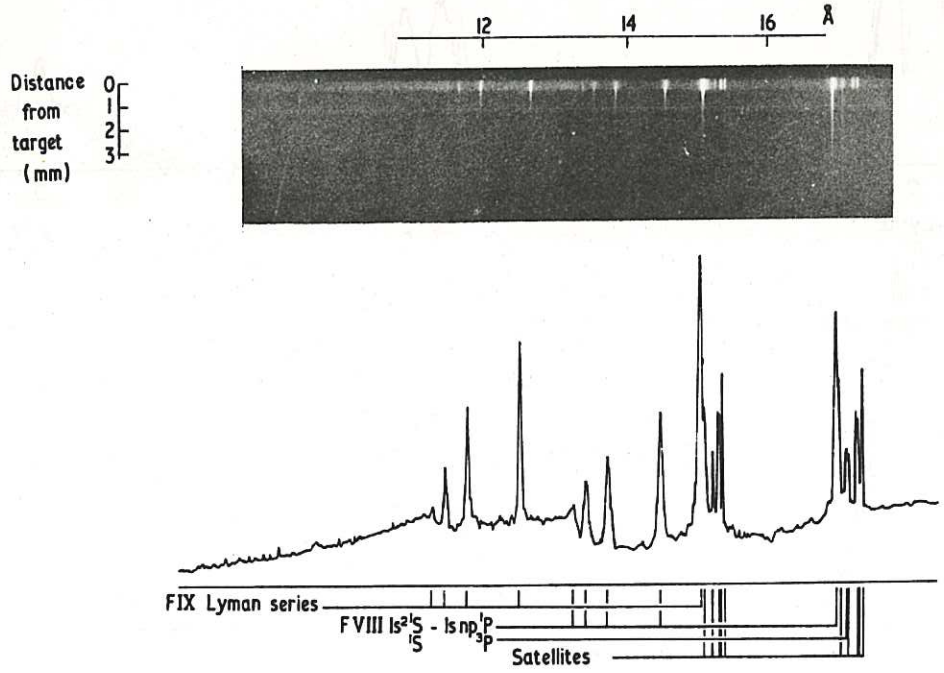

Fig.3 The Lyman spectrum of FIX and the FVIII resonance series in the plasma produced by laser irradiation of P.T.F.E. Also shown is a microphotometer scan taken close to the original target surface.

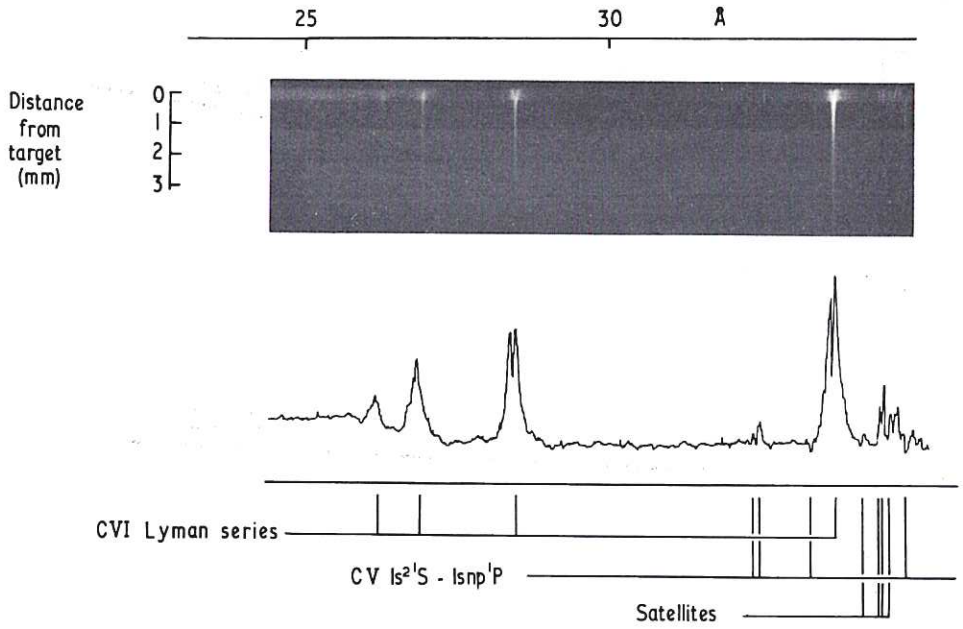

Fig.4 The Lyman spectrum of CVI in the plasma produced by laser irradiation of polythene. Also shown is a microphotometer scan taken close to the original target surface.

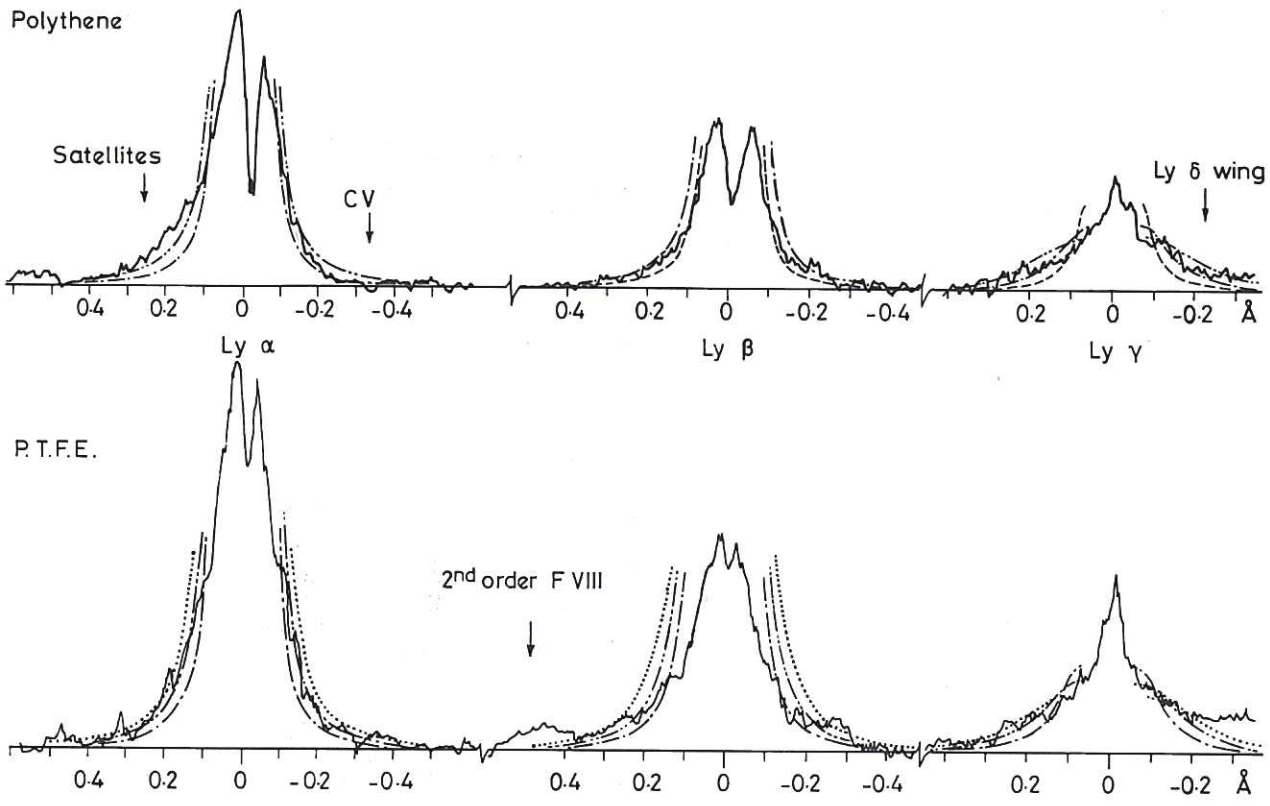

Fig.5 Microphotometer scans of the CVI Lyman lines. Theoretical predictions of photographic density in the line wings are shown for several values of E_0: – – – 2.10^5; –·–·– 3.10^5; –··–··– 4.10^5; ..... 5.10^5 (C.G.S. units). The first two series members show self reversal, with peak intensities much less than that predicted from line broadening in the wings, due to opacity. Other emission and absorption features are annotated.